MOLECULAR AND CELLULAR BIOLOGY, Sept. 1997, p. 5106–5116 Vol. 17, No. 9
0270-7306/97/$04.00+0

Multiple Interdependent Sequence Elements Control Splicing of a Fibroblast Growth Factor Receptor 2 Alternative Exon

FABIENNE DEL GATTO, ARIANE PLET, MARIE-CLAUDE GESNEL, CÉCILE FORT, AND RICHARD BREATHNACH*

INSERM U463, Institut de Biologie-CHR, 44093 Nantes Cedex 1, France

Received 25 March 1997/Returned for modification 20 May 1997/Accepted 5 June 1997

The fibroblast growth factor receptor 2 gene contains a pair of mutually exclusive alternative exons, one of which (K-SAM) is spliced specifically in epithelial cells. We have described previously (F. Del Gatto and R. Breathnach, Mol. Cell. Biol. 15:4825–4834, 1995) some elements controlling K-SAM exon splicing, namely weak exon splice sites, an exon-repressing sequence, and an intron-activating sequence. We identify here two additional sequences in the intron downstream from the K-SAM exon which activate splicing of the exon. The first sequence (intron-activating sequence 2 [IAS2]) lies 168 to 186 nucleotides downstream from the exon's 5′ splice site. The second sequence (intron-activating sequence 3 [IAS3]) lies 933 to 1,052 nucleotides downstream from the exon's 5′ splice site. IAS3 is a complex region composed of several parts, one of which (nucleotides 963 to 983) can potentially form an RNA secondary structure with IAS2. This structure is composed of two stems separated by an asymmetric bulge. Mutations which disrupt either stem decrease activation, while compensatory mutations which reestablish the stem restore activation, either completely or partially, depending on the mutation. We present a model for K-SAM exon splicing involving the intervention of multiple, interdependent pre-mRNA sequence elements.

Cells very often make several related yet distinct proteins from a single gene by alternative splicing of the corresponding pre-mRNA (36). This strategy can be exploited to express one form of a protein in some cell types and a different form in other cell types. One example of this behavior is provided by the fibroblast growth factor receptor 2 (FGFR-2) gene (28). The extracellular part of the receptor encoded by this gene is made up of three immunoglobulin-like domains. Two alternative exons, K-SAM and BEK, code for the carboxy-terminal half of the third, membrane-proximal, immunoglobulin-like domain (11). Splicing of the K-SAM exon generates a high-affinity receptor for FGF-1 and FGF-7, while splicing of the BEK exon generates a high-affinity receptor for FGF-1 and FGF-2 (38, 56). The splicing choice is strictly controlled, as certain cell types splice essentially only the K-SAM exon, while others splice essentially only the BEK exon (11, 38). As the splicing choice conditions the response of a cell to certain growth factors in its environment, the importance of strict control of splicing is evident during both development and adult life (40, 43).

Many other cases of alternative exon splicing have been described. For example, mouse c-*src* pre-mRNA contains two exons spliced only in neurons (7, 12, 39). The avian troponin T gene contains an optional exon spliced in the embryonic but not the adult heart (41, 54). Alpha- and beta-tropomyosin genes contain pairs of mutually exclusive internal exons spliced with strict tissue specificity (5, 14, 24, 25, 32). The pre-mRNA encoding calcitonin and calcitonin gene-related peptide contains six exons, one of which (exon 4) is skipped in a few cell types, including neuronal cells. As exon 4 is a terminal exon when spliced, this case is complicated by a possible link between polyadenylation and splicing. Indeed, it has recently been suggested that polyadenylation may be controlled here (33). Nevertheless, it is clear that mechanisms exist to control alternative splicing in a cell-type-specific manner and that these mechanisms are widely exploited.

The decision to splice an exon in one cell type but not in another can be made in different ways. Splicing of the exon may be specifically repressed, for instance. Thus, binding of a multiprotein complex including the P-element somatic inhibitor protein and a protein similar to the mammalian splicing factor hnRNP A1 to an exon inhibitory element represses splicing of the *Drosophila melanogaster* P-element third intron in the soma (44, 45). In the *Drosophila* sex determination cascade, the sex-lethal (sxl) protein represses use of a male-specific 3′ splice site on the transformer (tra) pre-mRNA by binding to the upstream polypyrimidine sequence and blocking binding of the essential splicing factor U2AF (50). Sometimes, splicing of an exon is activated specifically in one cell type. Once again, the *Drosophila* sex determination cascade furnishes an example: a multiprotein complex including the tra protein binds to a female-specific exon and activates its splicing (3, 53).

In mammalian systems, less is known about the control of alternative splicing. It is clear, however, that binding of certain members of the SR family of splicing factors (35, 57) to exon enhancer sequences is required for splicing of a number of exons (31, 41, 47, 52, 54). However, exons may also contain sequences which inhibit their splicing (1, 2, 9, 15, 16). Intron sequences which activate splicing of flanking exons have been described (5, 7, 15, 27, 46). Other intron sequences can repress splicing (12, 23, 37). It has recently been shown that binding of SR proteins to an intronic repressor element inhibits use of an alternative 3′ splice site of a regulated adenovirus pre-mRNA by preventing recruitment of the U2 snRNP particle to the spliceosome (29), suggesting that SR proteins can activate or repress splicing depending on where they bind to the pre-mRNA. The notion that SR proteins contribute to control of alternative splicing is reinforced by observations that the relative amounts of the proteins ASF/SF2 and hnRNP A1 can

* Corresponding author. Mailing address: INSERM U463, Institut de Biologie-CHR, 9 Quai Moncousu, 44093 Nantes Cedex 1, France. Phone: 33 2 40 08 47 50. Fax: 33 2 40 35 66 97. E-mail: breathna@nantes.inserm.fr.

influence the use of alternative splice sites both in vivo and in vitro (8, 21, 30, 34, 55).

It is clear from the examples discussed above that there is scope for complex regulation of exon splicing, a given exon being subject potentially to both activation and repression by multiple sequence elements present in both exon and intron sequences. In our previous work on the FGFR-2 system (15, 16, 22), we identified and characterized a sequence within the K-SAM exon which represses its splicing. We also identified a region of the downstream intron which activates K-SAM exon splicing. However, most of this downstream intron sequence was not analyzed. We complete here our analysis of the elements needed for K-SAM exon splicing and show that efficient K-SAM exon splicing requires the presence of multiple elements, two of which participate in formation of a secondary structure.

MATERIALS AND METHODS

Minigenes. The RK3 minigene has been described elsewhere (15). Many deletions were made by restriction enzyme digestion of RK3 followed by repair with the Klenow fragment of DNA polymerase I and religation by standard techniques (4). For example, minigenes of the b series were made by *Xho*I and *Hpa*I digestion. Minigenes Δ168–193, Δ194–214, mut 173–180, mut 181–188, and mut 189–193 were made by replacing an *Nco*I-*Xba*I fragment of RK3 with synthetic oligonucleotides as indicated in Fig. 1. Minigenes Δ859–932b, Δ859–943b, Δ859–963b, Δ859–983b, RK31b, Δ1053–1093b, Δ1033–1093b, Δ1021–1093b, Δ1011–1093b, Δ996–1093b, RK32b, RK33b, and RK37b were made by replacing the *Pst*I fragment (nucleotides 859 to 1093 [see Fig. 1]) of Δ1156–1233 with shorter fragments generated by PCR amplification, with RK3 as a template and suitable oligonucleotide primers. A minigene carrying an AAA-to-TTT mutation was made by replacing the *Nco*I-*Xba*I fragment of Δ194–214 by a double-stranded synthetic oligonucleotide of identical size carrying the desired mutation. A minigene carrying a TTT-to-AAA mutation was made by site-directed mutagenesis with the Transformer site-directed mutagenesis kit from Clontech. Minigenes of the mut 1 to mut 4 series were made by replacing an *Nco*I-*Xba*I fragment of Δ1156–1233 with mutated versions thereof. Minigenes of the mut 1′ to mut 4′ series, RK34b, RK35b, and RK36b, were made with the QuikChange site-directed mutagenesis kit from Stratagene. Mutations from each of the mut series were combined by restriction enzyme digestion and ligation of corresponding mutated minigenes. RK29b was made by introducing into the *Xba*I site of Δ859–1093b a fragment carrying IAS3. This fragment was obtained by PCR amplification with RK3 as a template with the oligonucleotides 5′-ACCACCACTAGTTGCAAACCAAAGCACAGG-3′ and 5′-CGAGAGAC TAGTAGCAACACTGACCAGCTC-3′, followed by *Spe*I digestion. RK30b was obtained similarly, except that the PCR fragment was introduced into the *Xba*I site of a minigene carrying deletions from nucleotides 168 to 193, 859 to 1093, and 1156 to 1233.

RT-PCR assay. SVK14 cells were stably transfected with minigenes, and RNA was harvested and analyzed by reverse transcription (RT)-PCR as described previously (15). Briefly, cDNA obtained by RT was amplified with a pair of primers flanking the alternative K-SAM and BEK exons. One of these primers is specific for the minigene. PCR products were digested with *Ava*I or *Hpa*I or left undigested before gel electrophoresis, Southern blotting, and hybridization with an FGFR-2 probe. Twenty cycles of PCR were used so as to remain within the exponential range of amplification. In consequence, Southern blotting was needed to visualize the PCR products and was carried out as described previously (15). Relative intensities of hybridizing fragments were analyzed with a Molecular Dynamics PhosphorImager.

Mung bean nuclease assay. The hybridization probe used was a 66-mer oligonucleotide whose sequence corresponded to antisense sequences of the 45 5′-most nucleotides of the C2 exon in the minigene and the 14 3′-most nucleotides of the K-SAM exon linked to the next 7 sense nucleotides of the K-SAM exon. The 5′ end of this probe could be protected only by minigene-derived RNA. The 66-mer was 5′ end labeled with [γ-^{32}P]ATP (6,000 Ci/mmol). Fifty micrograms of total RNA from transfected cells was hybridized to a large excess (10 fmol, 10^5 dpm) of probe in 30 μl of hybridization mixture (1 M NaCl, 0.17 M HEPES [pH 7.5], 0.33 mM EDTA) for 6 h at 55°C. Mung bean nuclease buffer (270 μl) and 50 U of mung bean nuclease (both from Life Technologies) were added before incubation for 45 min at 37°C. The reaction was stopped by ethanol precipitation, and protected probe fragments were subjected to electrophoresis on an 8% denaturing polyacrylamide gel. Radioactivity was detected and measured with a Molecular Dynamics PhosphorImager. Band intensity was determined after subtraction of the background obtained from a sample of untransfected SVK14 cell RNA analyzed in parallel. Each minigene was transfected independently at least twice. Each RNA sample was analyzed at least twice independently. Results presented are thus the averages of several independent determinations. For the relative splicing efficiency (RSE), the standard error was 3.5%.

RESULTS

The RK3 minigene (15) containing the alternative K-SAM and BEK exons together with flanking exons C1 and C2 is shown in Fig. 1A. Our experimental protocol involved stably transfecting minigenes into SVK14 cells (a human keratinocyte-derived cell line which normally splices the K-SAM exon), harvesting the RNA, and carrying out RT-PCR with primer P1 and the minigene-specific primer P2 (Fig. 1A). Splicing of the K-SAM or BEK exon yielded an amplified fragment of 0.46 kb with an *Ava*I or a *Hpa*I site, respectively, while skipping of both exons (splicing of C1 to C2) yielded an amplified fragment of 0.32 kb (Fig. 1B). PCR products were left undigested or digested with *Ava*I or *Hpa*I before electrophoresis on an agarose gel, transfer to a nylon membrane, and hybridization with a ^{32}P-labeled FGFR-2 cDNA fragment.

Localization of an intron sequence activating K-SAM exon splicing. Using RT-PCR and Northern blotting, we have previously shown (15) that at least two sequences downstream of the K-SAM exon are needed for efficient splicing of this exon. One of the two sequences (which we now call intron-activating sequence 1 [IAS1]) is a 20-nucleotide pyrimidine-rich sequence starting 10 nucleotides downstream from the 5′ splice site. The other sequence was only roughly defined and lies somewhere between a *Pst*I and an *Xba*I site of RK3, that is, in a region 80 to 214 nucleotides downstream of the 5′ splice site (Fig. 1A). We set out to localize with greater precision this sequence. Deletion of nucleotides 80 to 168 of RK3 (numbering here and henceforth refers to the distance downstream from the 5′ splice site of the K-SAM exon) did not reduce splicing of the K-SAM exon (Fig. 1C): 0.46-kb fragments with *Ava*I sites were obtained, while 0.32-kb fragments were scarcely detectable (<5%). However, deletion of nucleotides 169 to 214 led to reduced efficiency of splicing of the K-SAM exon, as evidenced by the generation of 0.32-kb fragments representing C1 spliced to C2 (30% of fragments). These results localized the activating sequence to a short *Nco*I-*Xba*I fragment (nucleotides 168 to 214 [Fig. 1A]). Deletion of the K-SAM exon proximal half (Δ168–193) of this fragment reduced the efficiency of K-SAM exon splicing, while deletion of the distal half (Δ194–214) had no detectable effect (Fig. 1A and C; note that the sequences shown in Fig. 1A are the residues which remain in the corresponding minigenes). These results localized the activating sequence within the nucleotide 168 to 193 region. The effects of various block mutations (mut 173–180, mut 181–188, and mut 189–193 [Fig. 1A]) in this region were tested. The results obtained (Fig. 1C) allowed us to define the activating sequence (intron-activating sequence 2 [IAS2]) as lying within the 21-bp sequence 5′-CCATGGAA AAATGCCCACAAC-3′.

Note that in some experiments (involving minigenes Δ169–214, Δ168–193, mut 173–180, and mut 181–188) a small fraction of 0.46-kb fragments were not cut by *Ava*I. This is probably the result of an incomplete digest, as we showed by sequencing eight subcloned 0.46-kb fragments which remained after *Ava*I digest.

A third intron sequence needed for efficient K-SAM exon splicing. Do additional activating sequences exist in the intron between the K-SAM and BEK exons? To answer this question, a series of further intron deletions was tested. Some of these deletions (Δ1156–1233 and Δ1093–1331) removed, in addition to intron sequences, the BEK exon's 3′ splice site and associated polypyrimidine sequence. Another deletion (Δ1156–1412)

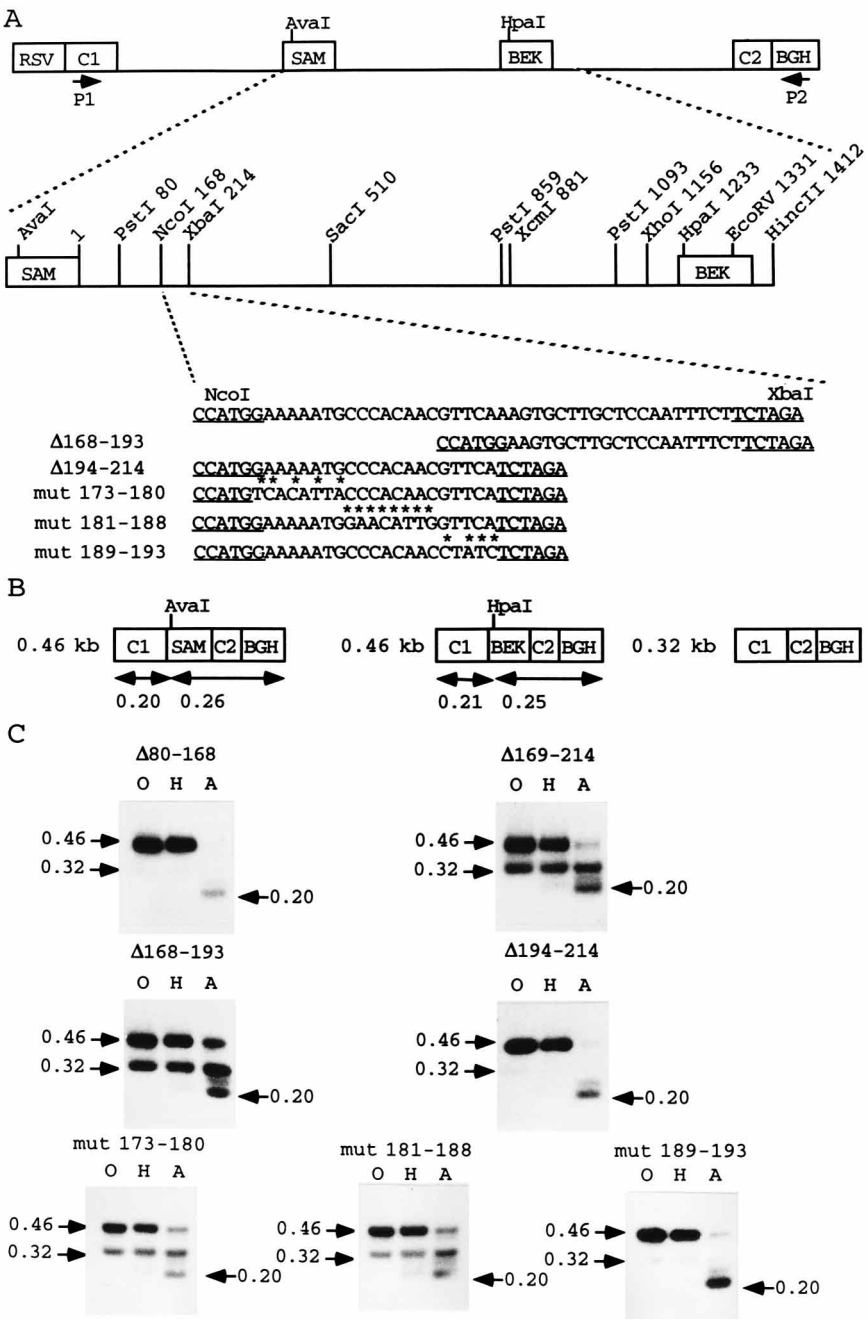

FIG. 1. Definition of an activating sequence in the intron downstream of the K-SAM exon. (A) The RK3 minigene (15) with the Rous sarcoma virus long terminal repeat promoter (RSV), the bovine growth hormone polyadenylation signal (BGH), the alternative K-SAM and BEK exons, and the flanking constitutively spliced exons C1 and C2 are shown. The alternative exons are 0.15 kb in size. The intron between exons C1 and K-SAM is 1.15 kb, the intron between exons K-SAM and BEK is 1.22 kb, and the intron between exons BEK and C2 is 1.9 kb. Primers P1 and P2, used for the PCR analysis, are indicated. Part of the region including the K-SAM and BEK exons is expanded, and sites for restriction enzymes used are shown. Numbering is from the first nucleotide (+1) of the intron downstream of the K-SAM exon. The nucleotide sequence of an *Nco*I-*Xba*I fragment (nucleotides 168 to 214) is shown, together with deleted or deleted and mutated versions thereof (asterisks mark mutated nucleotides) present in the minigenes used. For each minigene, the sequence which remains between the *Nco*I and *Xba*I sites is given. (B) Structures of PCR products and sizes, in kilobases, of their digestion products. (C) RT-PCR analysis of RNA from minigenes stably transfected into SVK14 cells. PCR products were left undigested (O) or digested with *Hpa*I (H) or *Ava*I (A) before Southern blotting. Autoradiograms of blots are shown. The sizes of certain fragments are given, in kilobases.

removed the entire BEK exon (Fig. 1A). These deletions thus rendered BEK exon splicing impossible. However, none of these deletions had a detectable effect on K-SAM exon splicing (Fig. 2). The analysis of results was now simpler, as the 0.46-kb fragment represented K-SAM exon splicing only. A comparison of the intensities of the 0.46-kb (SAM inclusion) and 0.32-kb (SAM exclusion) fragments thus allowed a direct measure of the effect of deletions on K-SAM exon splicing. To profit from this simpler analysis, further intron sequences were deleted from minigenes carrying the nucleotide 1156 to 1233

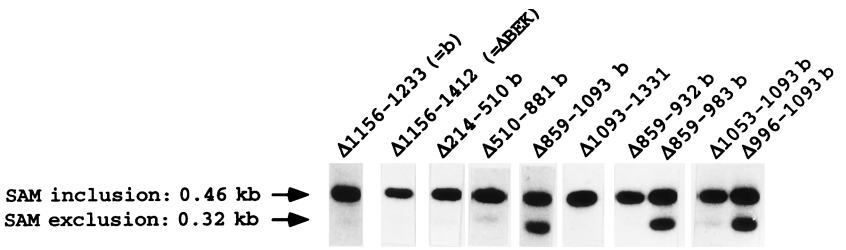

FIG. 2. An additional activating sequence lies 0.9 to 1.0 kb downstream from the K-SAM exon. An RT-PCR analysis of RNA from minigenes carrying indicated intron deletions stably transfected into SVK14 cells is shown.

deletion (henceforth minigenes carrying the nucleotide 1156 to 1233 deletion in addition to other deletions will be identified by the letter b). While deletion of nucleotides 214 to 510 or 510 to 881 had no detectable effect on K-SAM exon splicing (Fig. 2), deletion of nucleotides 859 to 1093 led to significant skipping of the K-SAM exon (0.32-kb fragments now represented 35% of PCR products). Very similar results were obtained when we analyzed the effect of deletion of nucleotides 859 to 1093 in a minigene containing an intact BEK exon, except that we now observed a low level of splicing of the BEK exon (data not shown).

Shorter deletions within the nucleotide 859 to 1093 region in minigenes lacking the BEK exon's 3′ splice site were tested for their effect on K-SAM exon splicing. Deleting nucleotides 859 to 932 or 1053 to 1093 had no detectable effect. However, deletion of nucleotides 859 to 983 or 996 to 1093 led to a level of K-SAM exon exclusion similar to that obtained with Δ859–1093 (Fig. 2). These results allowed us to localize an additional activating sequence (intron-activating sequence 3 [IAS3]) somewhere in the nucleotide 933 to 1052 region.

We used a mung bean nuclease assay to confirm the RT-PCR results described above. A 5′-end-labeled 66-mer oligonucleotide probe complementary to minigene RNA was hybridized to RNA from transfected cells, and the hybrids were treated with mung bean nuclease. Splicing of the K-SAM or C1 exon's 5′ splice site to the C2 exon's 3′ splice site should yield protected probe fragments of 59 and 49 nucleotides, respectively (Fig. 3A). Results obtained for several minigenes are shown in Fig. 3B. For all minigenes tested, two families of protected fragments were found: a first family of 47 to 51 nucleotides and a second family of 59 to 63 nucleotides (as well as traces of undigested probe). We have been unable to find conditions where single bands of 59 and 49 nucleotides were obtained. We interpret the results as follows. The family of 47 to 51 nucleotides represents RNAs in which the K-SAM exon has not been spliced to the C2 exon. Thus this family was detected exclusively when RNA from cells transfected with RK18 was analyzed (data not shown). We have demonstrated previously (15) that RK18 (which carries a deletion removing both IAS1 and IAS2) yields mainly C1-C2 RNA, with a small amount of BEK-C2 RNA, but no detectable RNA with K-SAM spliced to C2. The 59- to 63-nucleotide family represents RNA in which the K-SAM exon has been spliced to the C2 exon. The multiplicity of bands for each family reflects incomplete nuclease digestion (increasing the amount of nuclease used redistributes band intensity among members of this family but also leads to decreased overall signal). A comparison of the relative intensities of the two families is a measure of the amounts of K-SAM exon inclusion and exclusion.

For the Δ1156–1233 minigene, the results of the mung bean nuclease analysis were 85% K-SAM exon inclusion and 15% exclusion (Fig. 3B). The RT-PCR result was <5% exclusion. Note that the RT-PCR experiment compared K-SAM–C2 splicing to C1-C2 splicing, while the mung bean nuclease experiment compared K-SAM–C2 splicing to events which may include C1-C2 splicing, splicing of cryptic 5′ splice sites to C2, and retention of the intron upstream of the K-SAM exon (Fig. 3A). Events of the latter two types may have escaped detection in the RT-PCR analysis (long templates poorly amplified relative to the shorter K-SAM–C2 and C1-C2 templates, for example). Such events may be observed with the minigene because the C2 exon is incomplete; in particular, its 5′ splice site is lacking.

Splicing of the K-SAM exon as determined by the mung bean nuclease assay was reduced for minigenes lacking IAS2 (Δ168–193b, 51%) or IAS3 (Δ859–1093b, 55%) relative to results obtained with the Δ1156–1233 minigene (85%). As what is informative is not the absolute value of the K-SAM exon's splicing efficiency for a given mutated minigene but rather a comparison of this value to that obtained for the unmutated parent minigene, we shall henceforth cite the RSE. (The RSE is the K-SAM exon's splicing efficiency for a mutated minigene divided by the K-SAM exon's splicing efficiency for the parent Δ1156–1233 minigene times 100%). This method has an added advantage: if a small fraction of the C1-C2 signal for all minigenes were for some reason derived from the K-SAM–C2 signal by nuclease overdigestion, this might change slightly the absolute splicing efficiency for all minigenes but would have no effect on the relative splicing efficiency. For minigenes Δ168–193b and Δ859–1093b, the RSE was 60 and 65%, respectively. As determined by the RT-PCR analysis, the splicing efficiency of the K-SAM exon for these minigenes relative to that observed for the Δ1156–1233 minigene was approximately 65%. Conclusions drawn from the mung bean nuclease and RT-PCR assays are thus in good agreement.

IAS3 is composed of multiple elements. For minigenes Δ859–932b and Δ859–983b the RSE of the K-SAM exon as determined by the mung bean nuclease assay was 101 and 81%, respectively, while for minigenes Δ1053–1093b and Δ996–1093b the RSE was 99 and 76%, respectively. We constructed a variety of additional minigenes containing mutations in the region lying between bp 933 and 1052. Within this region (Fig. 4) there is an AAGAGAA sequence, similar to an ASF/SF2 consensus binding sequence (48); a TGCATG motif, known to activate splicing of a fibronectin gene exon (27); the sequence TAGG, which we have shown to repress splicing of the K-SAM exon when located within exon sequences (16); and two sequences similar to 5′ splice sites. These sequences were mutated. In addition, several deletion mutants were constructed. The resulting minigenes were transfected into SVK14 cells, and the RNA was analyzed with the mung bean nuclease assay. The results are summarized in Fig. 4, and some typical results are shown in Fig. 3B.

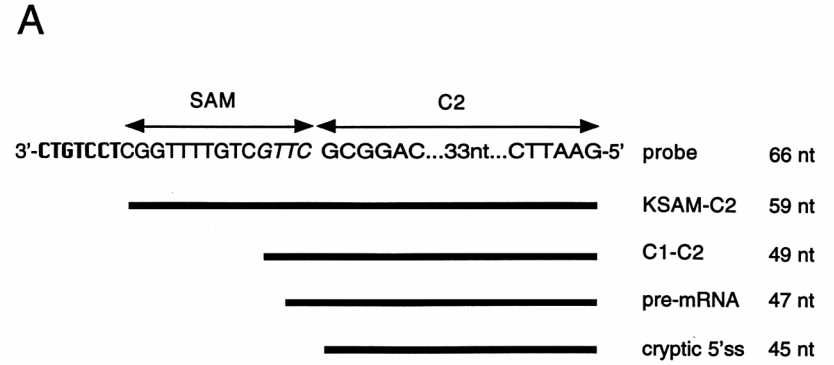

B

minigene	% SAM	RSE
none	-	-
Δ1156-1233	85	100
Δ168-193b	51	60
Δ859-1093b	55	65
Δ859-1093b+ Δ168-193b	51	60
Δ859-932b	86	101
Δ859-983b	69	81
Δ1053-1093b	84	99
Δ996-1093b	65	76
Δ1011-1093b	86	101
RK32b	63	73

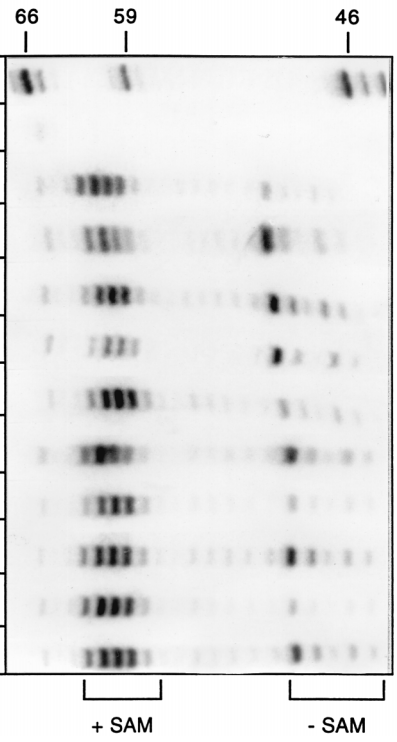

FIG. 3. Mung bean nuclease assay. (A) Structure of the 66-mer probe and sizes of the fragments thereof which can be protected by various minigene transcripts. "Cryptic 5′ ss" refers to the possible splicing of 5′ splice sites other than those of the K-SAM or C1 exon to the C2 exon's 3′ splice site. Nucleotides encoded by the K-SAM and C2 exons are indicated by arrows. Four nucleotides of the K-SAM exon which are also found at the 3′ end of the C1 exon are in italics. Seven nucleotides not encoded by the K-SAM exon are in boldface. (B) Mung bean nuclease assay results for RNA samples from SVK14 cells stably transfected with different mutated minigenes. M, markers of 66, 59, and 46 nucleotides; +SAM, bands attributed to K-SAM–C2 transcripts; −SAM, bands attributed to transcripts in which the K-SAM exon has not been spliced to the C2 exon; % SAM, ratio of +SAM band intensities to the sum of +SAM and −SAM band intensities multiplied by 100%; RSE, splicing efficiency of the K-SAM exon for a given mutated minigene relative to the splicing efficiency (85%) for the parent minigene, Δ1156–1233, multiplied by 100%.

The deletion analysis suggests that the upstream boundary of the activating sequence lies between nucleotides 943 and 963 (compare Δ859–943b and Δ859–963b), while the downstream boundary lies between nucleotides 1021 and 1033 (compare Δ1033–1093b and Δ1021–1093b). A negatively acting element may exist between nucleotides 1011 and 1021, as the RSE found for the Δ1021–1093b minigene (89%) was lower than that found for the Δ1011–1093b minigene (100%) despite the fact that the latter minigene had a larger deletion. An even larger deletion (Δ996–1093b) reduced the RSE to 76%, suggesting the presence of positively acting sequences between nucleotides 996 and 1011. This region contains the TGCATG and TAGG motifs referred to above. Mutation of the TAGG or TGCATG motif in the Δ1011–1093b minigene reduced the RSE from 101 to 92% (RK33b) or 73% (RK32b), respectively. However, mutation of the TAGG sequence (RK35b) or the TGCATG motif (RK34b) in the Δ1156–1233 minigene had little effect on the RSE. These results suggest that the TGCATG motif is important for activation but that there is a redundant sequence elsewhere, downstream of nucleotide 1011. Mutation of the ASF/SF2-like sequence had no detectable effect on the RSE (compare RK31b and Δ859–932b).

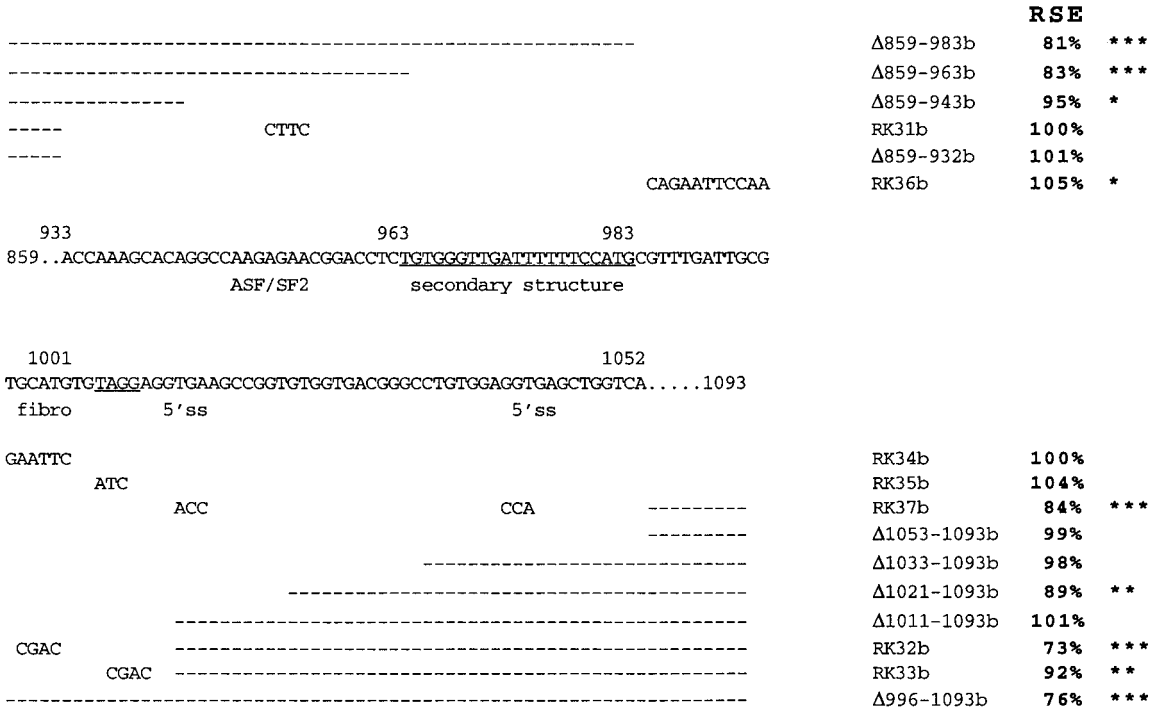

FIG. 4. Identification of some IAS3 elements needed for efficient K-SAM exon splicing. The nucleotide sequence of the intron downstream from the K-SAM exon from positions 933 to 1052 is shown. ASF/SF2, sequence resembling an ASF/SF2 consensus binding site (48); secondary structure, part of IAS3 which can participate in formation of a secondary structure with IAS2; fibro, hexamer known to activate splicing of a fibronectin alternative exon (27); 5′ ss, 5′ splice-site-like sequence. Numbering is as in Fig. 1. The extent of deletions present in different minigenes is shown by dashed lines. For appropriate minigenes, mutated nucleotides are shown. For each minigene, the RSE of the K-SAM exon as determined by the mung bean nuclease assay is given. Results for mutated minigenes were compared to that obtained for the parent minigene, Δ1156–1233, by using Fisher and Yates' reduced error test applicable to small samples (20a). Mutated minigenes are assigned one, two, or three asterisks according to the probability (*P*) that they in fact behave indistinguishably from the parent minigene (*, $P < 0.05$; **, $P < 0.01$; ***, $P < 0.001$).

However, simultaneous mutations of the two 5′ splice-site-like sequences reduced the RSE to 84% (RK37b).

The minimal indispensable region for activating K-SAM exon splicing thus exceeds nucleotides 963 to 1021. Within this region are grouped together several sequences controlling K-SAM exon splicing. However, the presence of redundant sequence elements outside this region is quite possible, and this prevents us from defining with greater precision the boundaries of IAS3.

IAS2 and part of IAS3 participate in a secondary structure. We noticed that part of IAS3 (nucleotides 963 to 983 [Fig. 4]) is imperfectly complementary to IAS2. IAS2 and IAS3 potentially participate in a structure composed of two RNA duplex regions or stems separated by an asymmetric bulge (Fig. 5A) and immediately followed by the other IAS3 sequences necessary for efficient K-SAM exon splicing. If IAS2 and IAS3 form this structure in vivo to activate K-SAM exon splicing, deleting both IAS2 and IAS3 should not have an additive effect on splicing. This was indeed the result obtained (Δ859–1093b plus Δ168–193b; compare to Δ859–1093b and Δ168–193b [Fig. 3B]).

Further evidence for the existence of the secondary structure was obtained by using minigenes carrying mutations designed to disrupt the stems of the structure. Replacing three A residues by three U residues in IAS2 (mut 1) or replacing three U residues by three A residues in IAS3 (mut 1′) disrupted stem 1 and led, respectively, to RSEs of 66 and 74% (Fig. 5B). However, when the minigene mut 1 + 1′, containing both of these replacements (and in which the stem can be reestablished, albeit with a different sequence), was used, the RSE obtained (103%) was essentially the same as that obtained with the parental minigene, Δ1156–1233 (100%). A similar conclusion was drawn from the RT-PCR approach (Fig. 5C). Further replacements designed to disrupt stem1, mut 2 and mut 2′, also reduced the RSE, to 56 and 13%, respectively. When both mutations were combined (mut 2 + 2′) to allow stem 1 to form again, the RSE increased to 76%. The marked reduction observed with mut 2′ relative to mut 2 may have been caused by the creation of the sequence UGCAUG in mut 2′. This sequence is known to be involved in controlling the splicing of some exons (27) and presumably represents a protein binding site. Such a protein may bind inappropriately to the mut 2′ pre-mRNA and interfere with splicing. When the mut 2 and mut 2′ mutations are combined, the UGCAUG sequence is hidden in a stem and is unavailable for protein binding. Mutations designed to disrupt stem 2 (mut 3, mut 3′, mut 4, and mut 4′) all reduced the RSE, while combining mutations mut 3 and mut 3′ or mut 4 and mut 4′ to reestablish stem 2 led to partial or complete recovery of the RSE.

The only reasonable explanation we can furnish for the above results is that IAS2 and part of IAS3 do indeed participate in formation of a secondary structure involved in activation of K-SAM exon splicing. However, complementarity alone cannot fully account for the results obtained. Thus, while reestablishing stem 1 or stem 2 in mutated minigenes always increased the RSE, the result obtained did not always approach 100% and mutations in IAS2 did not always have the same effect as corresponding mutations in IAS3. Perhaps in addition to the secondary structure, individual bases of IAS2 and IAS3 are recognized during the activation process.

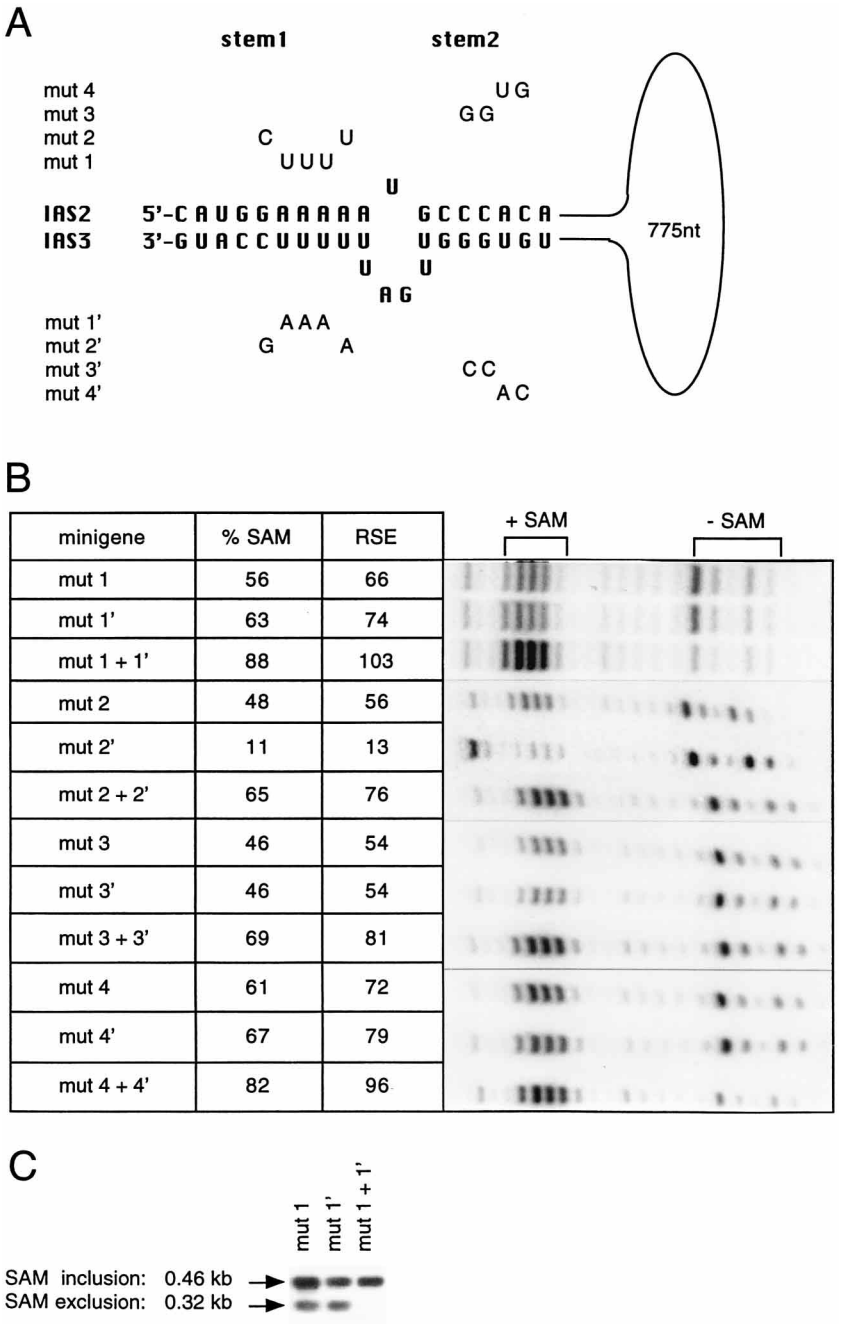

FIG. 5. IAS2 and part of IAS3 form a secondary structure needed for efficient K-SAM exon splicing. (A) Possible secondary structure formed in the pre-mRNA from the unmutated minigenes involving IAS2 (nucleotides 169 to 186) and IAS3 (nucleotides 963 to 983). Corresponding sequences for pre-mRNAs from mutated minigenes are also shown (only the mutated nucleotides are marked). (B) Mung bean nuclease assay results, as described in the legend to Fig. 3B. (C) RT-PCR analysis of RNA from SVK14 cells transfected with mut 1, mut 1′, and mut 1 + 1′.

It is interesting to note that some mutations in IAS3 which disrupt the secondary structure (mut′ series) can reduce the RSE more effectively than a mutation (Δ859–983b) which deletes completely that part of IAS3 involved in the secondary structure (Fig. 4 and 5). Perhaps incomplete formation of the secondary structure is actually deleterious. Note also that a deletion (Δ859–983b) which removes IAS3 sequence complementary to IAS2 and some upstream sequences and another deletion (Δ996–1093b) which removes the rest of IAS3 (including the 5′ splice-site-like sequences and the TGCATG motif) and some downstream sequences reduced the RSE to 81 and 76%, respectively, while combining the two deletions (Δ859–1093b) reduced the RSE to 65%, a value close to that obtained by deletion of IAS2. This additive effect suggests that the part of IAS3 involved in the secondary structure may act independently of the rest of IAS3.

The role of IAS2 is not limited to bringing IAS3 closer. One of the consequences of formation of the secondary structure is to bring IAS3 much closer to the K-SAM exon. If this were the sole function of the secondary structure, IAS3 should function

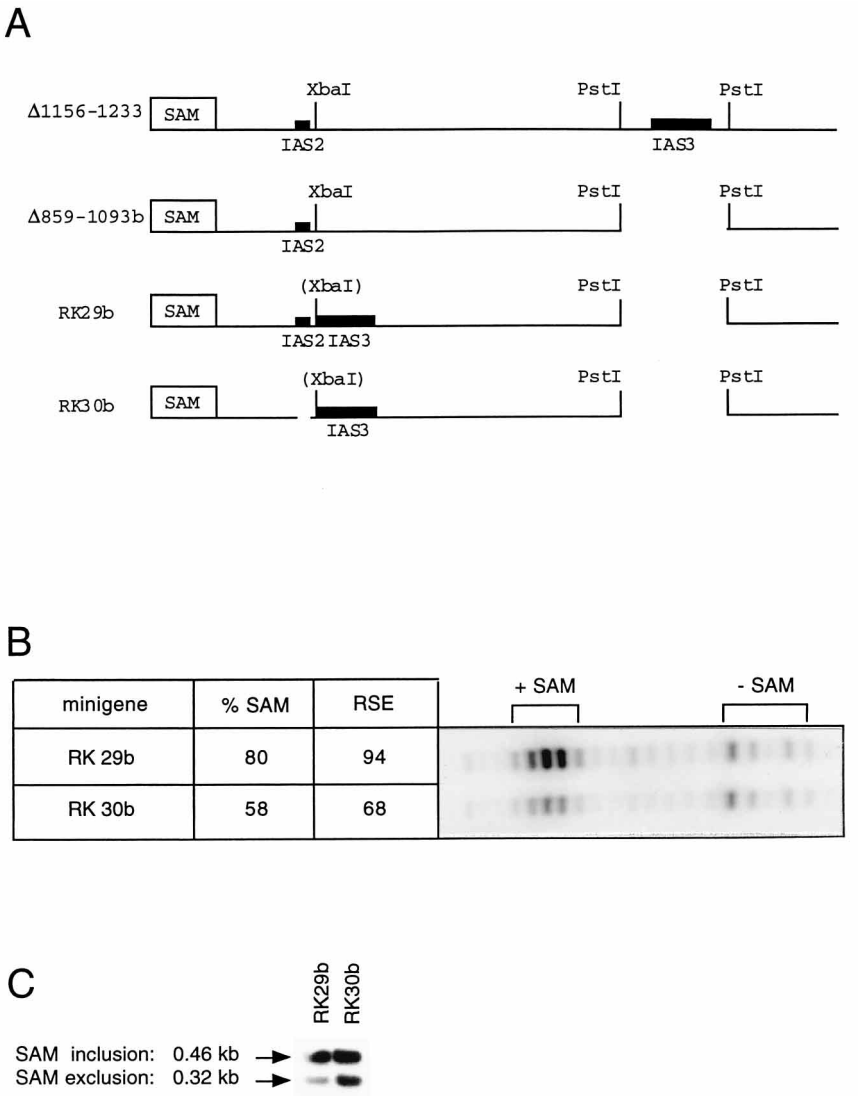

FIG. 6. IAS2 is still needed even when IAS3 is brought closer to the K-SAM exon. (A) Structures of parts of the minigenes tested. In RK29b, IAS3 has been placed immediately after the nucleotide 168 to 214 *Nco*I-*Xba*I fragment containing IAS2 (Fig. 1). In RK30b, nucleotides 168 to 193, containing IAS2, have been deleted from RK29b. (B) Mung bean nuclease analysis of RNA from the minigenes shown in panel A stably transfected into SVK14 cells. (C) RT-PCR analysis of RNA from SVK14 cells transfected with RK29b and RK30b.

in the absence of IAS2 if placed in the position normally occupied by IAS2. However, results presented in Fig. 6 show that this is not the case. In pre-mRNA from Δ1156–1233, IAS2 and IAS3 were both present and the secondary structure formed normally. In Δ859–1093b, IAS3 was absent. This absence led to a reduced RSE (65%). When IAS3 was reintroduced into Δ859–1093b in a position immediately behind IAS2 (minigene RK29b), the secondary structure still formed, although with only 68 nucleotides between IAS2 and IAS3. The RSE increased to 94%. When IAS2 was removed from minigene RK29b by deletion of bp 168 to 193, the RSE decreased to 68% (RK30b), a level similar to that observed (60%) with the minigene Δ168–193b, in which IAS3 is in its normal position. Similar results were obtained with the RT-PCR assay (Fig. 6C). Thus, bringing IAS3 closer to the K-SAM exon is not sufficient in itself to fully activate splicing in the absence of IAS2.

That IAS2 does not uniquely serve to reposition IAS3 is in agreement with our other results. Thus, deletion of IAS2 (Δ168–193b) yielded an RSE of 60%, while deletion of a part of IAS3 containing the sequences complementary to IAS2 (Δ859–983b) yielded an RSE of 81% (Fig. 4). However, deletion of all of IAS3 (Δ859–1093b) reduced the RSE to 65%, a value similar to that obtained by deletion of IAS2. Furthermore, the IAS3 and IAS2 deletions did not have an additive effect. These results are in agreement with a model in which IAS2 helps all the various parts of IAS3 to work.

DISCUSSION

We describe here two sequences involved in controlling splicing of the K-SAM alternative exon of the human FGFR-2 gene. Both sequences lie in the intron downstream from the K-SAM exon, 168 to 185 bp (IAS2) and 933 to 1,052 bp (IAS3) downstream from this exon's 5′ splice site. Mutation of IAS2 or IAS3 can lead to skipping of the K-SAM exon in about one

mRNA in three in cells which normally splice this exon. This does not solely imply a decrease in functional mRNA levels, as skipping of the K-SAM exon yields mRNAs potentially coding for secreted FGFR-2 molecules, which contain the first two immunoglobulin-like domains but only half of the third immunoglobulin-like domain. These truncated molecules may interfere with the normal function of the intact receptors. The contribution of IAS2 and IAS3 may thus be particularly important in the biological context of the FGFR-2 gene.

IAS3 is a complex region composed of several different elements. Thus, part of IAS3 can participate with IAS2 in the formation of a secondary structure in the pre-mRNA. Formation of this secondary structure is involved in activating splicing of the K-SAM exon. Mutations in IAS2 or IAS3 which disrupt stems of the secondary structure reduce the splicing efficiency of the K-SAM exon by 30 to 50%, while compensatory mutations which reestablish the stems restore splicing completely or partially. In addition to containing sequences complementary to IAS2, IAS3 contains other sequences activating splicing, among which we have been able to identify the sequence UGCAUG, known to activate splicing in other genes (27), and one or two 5′ splice-site-like sequences. The several sequences grouped together in IAS3 may act independently or semi-independently.

What does the secondary structure do, and how is it formed? It is known that formation of a secondary structure involving sequences between the branch site and the 3′ splice site can facilitate the use of branch sites which are unusually distant from the corresponding 3′ splice sites (10, 13, 17). This suggested that our secondary structure might work in a similar fashion, its role limited to bringing IAS3 and flanking sequences closer to the K-SAM exon. This does not appear to be the case, however, as bringing these sequences closer to the K-SAM exon is not enough to activate splicing in the absence of IAS2.

Some other examples of secondary structures which influence exon splicing have been described in the literature. For example, exon sequences forming a secondary structure favor the use of the natural 5′ splice site of adenovirus 2 E3 pre-mRNA relative to that of a cryptic site 74 nucleotides downstream (18). On the other hand, sequestering splice sites in secondary structures can hinder exon splicing, as observed for example for the chicken beta-tropomyosin transcript (6, 14, 32) and the human growth hormone transcript (20). Binding of a ribosomal protein to a secondary structure formed by exon sequences of its own pre-mRNA can block splicing by hindering association of U2 snRNP (51). However, in these examples, the connecting loops of the secondary structures are relatively short. Indeed, with an artificially generated stem used to sequester a 5′ splice site, it has been shown that loop size has important consequences for the effect on splicing: inhibition of splicing is observed only if the loop is smaller than 50 to 55 nucleotides (19). This indicates that the secondary structure does not form in vivo if the loop size is greater than about 50 nucleotides. In our case, IAS2 and the IAS2-complementary sequences of IAS3 are separated by around 800 nucleotides. It is thus quite unlikely that the secondary structure forms spontaneously. A more likely hypothesis is that formation of the structure is assisted by proteins involved in splicing.

What the secondary structure does and how it forms are thus questions which may only be answered if splicing of the K-SAM exon is considered as a whole. Taken together with our previously published findings (15, 16, 22), the results described here show that splicing of the K-SAM exon is a complex phenomenon. At least six elements are involved (Fig. 7). Two of these elements are the exon's weak 3′ and 5′ splice sites. A

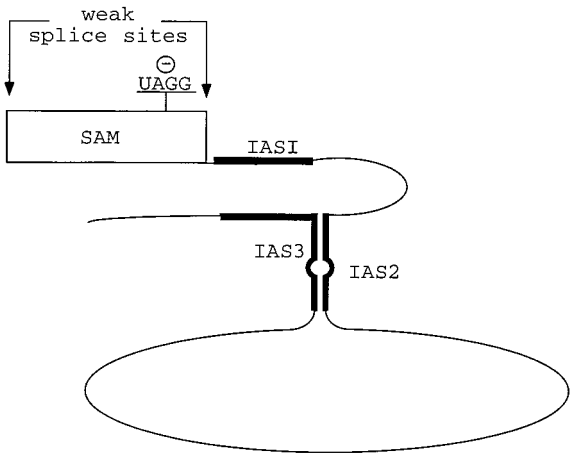

FIG. 7. Schematic representation of sequence elements controlling K-SAM exon splicing.

third element is the short exon sequence UAGG, which represses splicing of the K-SAM exon. The fourth element is a splice-activating sequence rich in pyrimidines starting 10 nucleotides downstream from the K-SAM exon's 5′ splice site (IAS1). The two elements described here, IAS2 and IAS3, also activate K-SAM exon splicing. The K-SAM exon is spliced efficiently in SVK14 cells but not in HeLa cells (11). This could be explained conveniently were the exon-repressing sequence to work only in HeLa cells and the intron-activating sequences to work only in SVK14 cells. To test this hypothesis rigorously it is necessary to analyze the effects of mutations in these sequences in both HeLa and SVK14 cells in the context of the intact minigene. We have tried to study the effects of mutations in IAS1, IAS2, and IAS3 in HeLa cells. Unfortunately the level of K-SAM exon splicing in HeLa cells, even with a minigene lacking the BEK exon, is too low to allow this analysis (our unpublished results).

The six elements we have identified are interdependent. Thus, IAS2 and IAS3 function at least in part together. In the absence of the exon-repressing sequence, or if the 5′ or 3′ splice sites are brought closer to the corresponding consensus sequences, IAS1 and IAS2 are no longer needed for efficient K-SAM exon splicing (15). On the other hand, the exon-repressing sequence no longer works if the splice sites are reinforced (15). As we have shown previously, mutation of IAS1 has a drastic effect in SVK14 cells on K-SAM exon splicing, which is reduced by at least 95%, although IAS2 and IAS3 remain intact. Mutation of IAS2 or IAS3 in a minigene containing intact IAS1 reduces splicing by 30 to 50%. These results suggest a model in which the role of IAS2 and IAS3 is to confer full activity on IAS1. Based on all of the above observations, we propose, as a speculative model for K-SAM exon splicing, that proteins bound to IAS1 can only partially overcome the negative effect on K-SAM exon splicing of the exon-repressing sequence, which may function to block a necessary dialogue (26, 42) between the exon's weak splice sites. Perhaps proteins bound to IAS2 and IAS3 interact, bringing IAS2 and IAS3 closer together; IAS2 and part of IAS3 can then form a secondary structure. This may be accompanied by either the loss of some proteins or the binding of additional proteins. The resulting complex of proteins bound to IAS1, IAS2, and IAS3 finally serves to counteract fully the effect of the repressing sequences within the K-SAM exon. Our model is, of course, formally identical to models currently proposed for the activa-

tion of transcription. Such models often invoke the establishment of contacts between proteins bound to sites which may be widely separated on the DNA, with the resulting multiprotein-nucleic acid complex (enhanceosome) interacting with the basal transcription machinery to activate transcription (49).

ACKNOWLEDGMENTS

This work was supported by grants from the Association pour la Recherche sur le Cancer and the Ligue Nationale contre le Cancer, Comité Departemental de Loire-Atlantique.

REFERENCES

1. **Amendt, B. A., D. Hesslein, L. J. Chang, and C. M. Stoltzfus.** 1994. Presence of negative and positive *cis*-acting RNA flanking elements within and flanking the first Tat coding exon of human immunodeficiency virus type 1. Mol. Cell. Biol. **14:**3960–3970.
2. **Amendt, B. A., Z.-H. Si, and C. M. Stoltzfus.** 1995. Presence of exon splicing silencers within human immunodeficiency virus type 1 *tat* exon 2 and *tat-rev* exon 3: evidence for inhibition mediated by cellular factors. Mol. Cell. Biol. **15:**4606–4615.
3. **Amrein, H., M. L. Hedley, and T. Maniatis.** 1994. The role of specific protein-RNA and protein-protein interactions in positive and negative control of pre-mRNA splicing by transformer 2. Cell **76:**735–746.
4. **Ausubel, F. M., R. Brent, R. E. Kingston, D. D. Moore, J. G. Seidman, J. A. Smith, and K. Struhl (ed.).** 1991. Current protocols in molecular biology. John Wiley and Sons, New York, N.Y.
5. **Balvay, L., D. Libri, M. Gallego, and M. Fiszman.** 1992. Intronic sequences with both positive and negative effects on the regulation of alternative splicing of the chicken beta-tropomyosin transcripts. Nucleic Acids Res. **20:**3987–3992.
6. **Balvay, L., D. Libri, and M. Y. Fiszman.** 1993. Pre-mRNA secondary structure and the regulation of splicing. Bioessays **15:**165–169.
7. **Black, D. L.** 1992. Activation of *c-src* neuron-specific splicing by an unusual RNA element in vivo and in vitro. Cell **69:**795–807.
8. **Caceres, J. F., S. Stamm, D. M. Helfman, and A. R. Krainer.** 1994. Regulation of alternative splicing by overexpression of antagonistic splicing factors. Science **265:**1706–1709.
9. **Caputi, M., G. Casari, S. Guenzi, R. Tagliabue, A. Sidoli, C. A. Melo, and F. E. Baralle.** 1994. A novel bipartite splicing enhancer modulates the differential processing of the human fibronectin EDA exon. Nucleic Acids Res. **22:**1018–1022.
10. **Cellini, A., E. Felder, and J. J. Rossi.** 1986. Yeast pre-messenger RNA splicing efficiency depends on critical spacing requirements between the branch-point and 3′ splice site. EMBO J. **5:**1023–1030.
11. **Champion-Arnaud, P., C. Ronsin, E. Gilbert, M. C. Gesnel, E. Houssaint, and R. Breathnach.** 1991. Multiple mRNAs code for proteins related to the BEK fibroblast growth factor receptor. Oncogene **6:**979–987.
12. **Chan, R. C., and D. L. Black.** 1995. Conserved intron elements repress splicing of a neuron-specific c-*src* exon in vitro. Mol. Cell. Biol. **15:**6377–6385.
13. **Chebli, K., R. Gattoni, P. Schmitt, G. Hildwein, and J. Stevenin.** 1989. The 216-nucleotide intron of the E1A pre-mRNA contains a hairpin structure that permits utilization of unusually distant branch acceptors. Mol. Cell. Biol. **9:**4852–4861.
14. **Clouet d'Orval, B., Y. d'Aubenton Carafa, P. Sirand-Pugnet, M. Gallego, E. Brody, and J. Marie.** 1991. RNA secondary structure repression of a muscle-specific exon in HeLa cell nuclear extracts. Science **252:**1823–1828.
15. **Del Gatto, F., and R. Breathnach.** 1995. Exon and intron sequences, respectively, repress and activate splicing of a fibroblast growth factor receptor 2 alternative exon. Mol. Cell. Biol. **15:**4825–4834.
16. **Del Gatto, F., and R. Breathnach.** 1996. The exon sequence TAGG can inhibit splicing. Nucleic Acids Res. **24:**2017–2021.
17. **Deshler, J. O., and J. J. Rossi.** 1991. Unexpected point mutations activate cryptic 3′ splice sites by perturbing a natural secondary structure within a yeast intron. Genes Dev. **5:**1252–1263.
18. **Domenjoud, L., H. Gallinaro, L. Kister, S. Meyer, and H. Jacob.** 1991. Identification of a specific exon sequence that is a major determinant in the selection between a natural and a cryptic 5′ splice site. Mol. Cell. Biol. **11:**4581–4590.
19. **Eperon, L. P., R. I. Graham, A. D. Griffiths, and I. C. Eperon.** 1988. Effects of RNA secondary structure on alternative splicing of pre-mRNA: is folding limited to a region behind the transcribing RNA polymerase? Cell **54:**393–401.
20. **Estes, P. A., N. E. Cooke, and S. A. Liebhaber.** 1992. A native secondary structure controls alternative splice-site selection and generates two human growth hormone isoforms. J. Biol. Chem. **267:**14902–14908.

20a. **Fisher, R. A., and F. Yates.** 1953. Statistical tables for biological, agricultural and medical research. Oliver and Boyd, Edinburgh, United Kingdom.

21. **Ge, H., and J. L. Manley.** 1990. A protein factor, ASF, controls cell specific alternative splicing of SV40 early pre-mRNA in vitro. Cell **62:**25–34.
22. **Gilbert, E., F. Del Gatto, P. Champion-Arnaud, M. C. Gesnel, and R. Breathnach.** 1993. Control of BEK and K-SAM splice sites in alternative splicing of the fibroblast growth factor receptor 2 pre-mRNA. Mol. Cell. Biol. **13:**5461–5468.
23. **Gontarek, R. R., M. T. McNally, and K. Beemon.** 1993. Mutation of an RSV intronic element abolishes both U11/U12 snRNP binding and negative regulation of splicing. Genes Dev. **7:**1926–1936.
24. **Gooding, C., G. C. Roberts, G. Moreau, B. Nadal-Ginard, and C. W. J. Smith.** 1994. Smooth muscle-specific switching of alpha-tropomyosin mutually exclusive exon selection by specific inhibition of the strong default exon. EMBO J. **13:**3861–3872.
25. **Graham, I. R., M. Hamshere, and I. C. Eperon.** 1992. Alternative splicing of a human α-tropomyosin muscle-specific exon: identification of determining sequences. Mol. Cell. Biol. **12:**3872–3882.
26. **Hoffman, B. E., and P. J. Grabowski.** 1992. U1 snRNP targets an essential splicing factor, U2AF65, to the 3′ splice site by a network of interactions spanning the exon. Genes Dev. **6:**2554–2568.
27. **Huh, G. S., and R. O. Hynes.** 1994. Regulation of alternative pre-mRNA splicing by a novel repeated hexanucleotide element. Genes Dev. **8:**1561–1574.
28. **Johnson, D. E., and L. T. Williams.** 1993. Structural and functional diversity in the FGF receptor multigene family. Adv. Cancer Res. **60:**1–41.
29. **Kanopka, A., O. Muhlemann, and G. Akusjarvi.** 1996. Inhibition by SR proteins of splicing of a regulated adenovirus pre-mRNA. Nature **381:**535–538.
30. **Krainer, A. R., G. C. Conway, and D. Kozak.** 1990. The essential pre-mRNA splicing factor SF2 influences 5′ splice site selection by activating proximal sites. Cell **62:**35–42.
31. **Lavigueur, A., H. La Branche, A. R. Kornblihtt, and B. Chabot.** 1993. A splicing enhancer in the human fibronectin alternate ED1 exon interacts with SR proteins and stimulates U2 snRNP binding. Genes Dev. **7:**2405–2417.
32. **Libri, D., A. Piseri, and M. Y. Fiszman.** 1991. Tissue-specific splicing in vivo of the beta-tropomyosin gene: dependence on an RNA secondary structure. Science **252:**1842–1845.
33. **Lou, H., R. F. Gagel, and S. M. Berget.** 1996. An intron enhancer recognized by splicing factors activates polyadenylation. Genes Dev. **10:**208–219.
34. **Mayeda, A., D. M. Helfman, and A. R. Krainer.** 1993. Modulation of exon skipping and inclusion by heterogeneous nuclear ribonucleoprotein A1 and pre-mRNA splicing factor SF2/ASF. Mol. Cell. Biol. **13:**2993–3001.
35. **Mayeda, A., A. M. Zahler, A. R. Krainer, and M. B. Roth.** 1992. Two members of a conserved family of nuclear phosphoproteins are involved in pre-mRNA splicing. Proc. Natl. Acad. Sci. USA **89:**1301–1304.
36. **McKeown, M.** 1992. Alternative mRNA splicing. Annu. Rev. Cell Biol. **8:**133–155.
37. **McNally, L. M., and M. T. McNally.** 1996. SR protein splicing factors interact with the Rous sarcoma virus negative regulator of splicing element. J. Virol. **70:**1163–1172.
38. **Miki, T., D. P. Bottaro, T. P. Fleming, C. L. Smith, W. H. Burgess, A. M. L. Chan, and S. A. Aaronson.** 1992. Determination of ligand-binding specificity by alternative splicing: two distinct growth factor receptors encoded by a single gene. Proc. Natl. Acad. Sci. USA **89:**246–250.
39. **Min, H., R. C. Chan, and D. L. Black.** 1995. The generally expressed hnRNP F is involved in a neural-specific pre-mRNA splicing event. Genes Dev. **9:**2659–2671.
40. **Orr-Urtreger, A., M. T. Bedford, T. Burakova, E. Arman, Y. Zimmer, A. Yayon, D. Givol, and P. Lonai.** 1993. Developmental localization of the splicing alternatives of fibroblast growth factor receptor-2 (FGFR-2). Dev. Biol. **158:**475–486.
41. **Ramchatesingh, J., A. M. Zahler, K. M. Neugebauer, M. B. Roth, and T. A. Cooper.** 1995. A subset of SR proteins activates splicing of the cardiac troponin T alternative exon by direct interactions with an exonic enhancer. Mol. Cell. Biol. **15:**4898–4907.
42. **Robberson, B. L., G. J. Cote, and S. M. Berget.** 1990. Exon definition may facilitate splice site selection in RNA with multiple introns. Mol. Cell. Biol. **10:**84–94.
43. **Sato, M., T. Kitazawa, A. Katsumata, M. Mukamoto, T. Okada, and T. Takeya.** 1992. Tissue-specific expression of two isoforms of chicken fibroblast growth factor receptor, bek and Cek3. Cell Growth Differ. **3:**355–361.
44. **Siebel, C. W., L. D. Fresco, and D. C. Rio.** 1992. The mechanism of somatic inhibition of drosophila P-element pre-mRNA splicing: multiprotein complexes at an exon pseudo-5′ splice site control U1 snRNP binding. Genes Dev. **6:**1386–1401.
45. **Siebel, C. W., R. Kanaar, and D. C. Rio.** 1994. Regulation of tissue-specific P-element pre-mRNA splicing requires the RNA-binding protein PSI. Genes Dev. **8:**1713–1725.
46. **Sirand-Pugnet, P., P. Durosay, E. Brody, and J. Marie.** 1995. An intronic (A/U)GGG repeat enhances the splicing of an alternative intron of the chicken beta-tropomyosin pre-mRNA. Nucleic Acids Res. **23:**3501–3507.
47. **Sun, Q., A. Mayeda, R. K. Hampson, A. R. Krainer, and F. M. Rottman.** 1993. General splicing factor SF2/ASF promotes alternative splicing by binding to an exonic splicing enhancer. Genes Dev. **7:**2598–2608.
48. **Tacke, R., and J. L. Manley.** 1995. The human splicing factors ASF/SF2 and

SC35 possess distinct, functionally significant RNA binding specificities. EMBO J. **14:**3540–3551.
49. **Thanos, D., and T. Maniatis.** 1995. Virus induction of human IFN beta gene expression requires the assembly of an enhanceosome. Cell **83:**1091–1100.
50. **Valcarel, J., S. Ravinder, P. D. Zamore, and M. R. Green.** 1993. The protein sex-lethal antagonizes the splicing factor U2AF to regulate alternative splicing of transformer pre-mRNA. Nature **362:**171–175.
51. **Villardel, J., and J. R. Warner.** 1994. Regulation of splicing at an intermediate step in the formation of the spliceosome. Genes Dev. **8:**211–220.
52. **Watakabe, A., K. Tanaka, and Y. Shimura.** 1993. The role of exon sequences in splice site selection. Genes Dev. **7:**407–418.
53. **Wu, J. Y., and T. Maniatis.** 1993. Specific interactions between proteins implicated in splice site selection and regulated alternative splicing. Cell **75:**1061–1070.
54. **Xu, R., J. Teng, and T. A. Cooper.** 1993. The cardiac troponin T alternative exon contains a novel purine-rich positive splicing element. Mol. Cell. Biol. **13:**3660–3674.
55. **Yang, X., M. R. Bani, S. J. Lu, S. Rowan, Y. Ben-David, and B. Chabot.** 1994. The A1 and A1B proteins of heterogeneous nuclear ribonucleoparticles modulate 5′ splice site selection in vivo. Proc. Natl. Acad. Sci. USA **91:**6924–6928.
56. **Yayon, A., Y. Zimmer, S. Guo-Hong, A. Avivi, Y. Yarden, and D. Givol.** 1992. A confined variable region confers ligand specificity on fibroblast growth factor receptors: implications for the origin of the immunoglobulin fold. EMBO J. **11:**1885–1890.
57. **Zahler, A. M., W. S. Lane, J. A. Stolk, and M. B. Roth.** 1992. SR proteins: a conserved family of pre-mRNA splicing factors. Genes Dev. **6:**837–847.